Modelling the biomass updraft gasification process using the combination of a pyrolysis kinetic model and a thermodynamic equilibrium model

Cerinski, Damijan; Ferreiro, Ana Isabel; Baleta, Jakov; Costa, Mário; Zimbardi, Francesco; Cerone, Nadia; Wang, Jin

Modelling the biomass updraft gasification process using the combination of a pyrolysis kinetic model and a thermodynamic equilibrium model

Damijan Cerinski [a], Ana Isabel Ferreiro [b], Jakov Baleta [a,*], Mário Costa [b], Francesco Zimbardi [c], Nadia Cerone [c], Jin Wang [d]

[a] Faculty of Metallurgy, University of Zagreb, Sisak, Croatia
[b] IDMEC, Mechanical Engineering Department, Instituto Superior Técnico, University of Lisbon, Lisbon, Portugal
[c] Department of Energy Technologies and Renewable Resources, ENEA, Rotondella, Italy
[d] School of Energy and Environmental Engineering, Hebei University of Technology, Tianjin, China

ABSTRACT

Conversion of biomass into gas suitable for further exploitation is one of the valuable renewable energy pathways due to the wide distribution and availability of raw materials. Biomass gasification is a thermochemical process of partial combustion in a reduced oxygen environment that aims to produce hydrogen-enriched syngas. Updraft gasifier design, with its advantages of high efficiency, produces syngas with higher hydrogen yield compared to other gasifier designs. The main drawback of the updraft gasifier is high yield of tars in the outflow gas decreasing its lower heating value. Recently, significant research efforts have focused on the optimization of the updraft gasifiers operating conditions, especially by developing numerical models as a complementary approach to experiments. The simplest modelling approach for predicting biomass gasification behaviour is the thermodynamic equilibrium model. When describing the behaviour of an updraft gasifier, special focus needs to be given to the pyrolysis stage, since in this type of reactor pyrolysis products directly outflow from the gasifier. In this work, a pilot-scale biomass gasifier was modelled using a combination of a pyrolysis kinetic model with a thermodynamic equilibrium model. To describe the pyrolysis behaviour, the CRECK-S-BIO and two secondary gas-phase mechanisms with distinct levels of complexity were used. The gasification and oxidation of char were modelled using a thermodynamic equilibrium model through the minimization of Gibbs free energy approach. The predicted results of dry clean syngas were compared to the experimental data considering eleven different operating conditions. The model combination that used the detailed secondary gas-phase mechanism achieved generally lower average prediction errors. Although some discrepancies were observed in the predictions, these preliminary results show that the model approach considered in this study represents a good basis for future development of the model.

1. Introduction

Climate changes caused by the release of greenhouse gases (GHG) into the atmosphere during the combustion of fossil fuels encouraged much more focus on the development of clean energy systems. Renewable energy sources include solar, wind, water and geothermal energy, as well as energy released from the thermal conversion of organic matter, such as biomass (Ishaq and Dincer, 2020). In the literature, various scenarios are proposed to determine the direction of developing clean energy systems, but the solution lies in the necessity of using all forms of renewable energy resources, especially when considering their intermittency (Zappa et al., 2019).

Using biomass as an energy resource has the advantages of wide distribution, availability of raw materials and, currently is one of the four most common energy resources with a 10% share of total world primary energy (Farzad et al., 2016). Biomass gasification is a thermochemical conversion process that works under a low oxygen environment, which mainly results in the conversion of biomass into a syngas suitable for further energy conversions, especially for the use in gas turbines, fuel cells and

* Corresponding author.
E-mail addresses: dcerinski@simet.unizg.hr (D. Cerinski), ana.ferreiro@tecnico.ulisboa.pt (A.I. Ferreiro), baleta@simet.unizg.hr (J. Baleta), francesco.zimbardi@enea.it (F. Zimbardi), nadia.cerone@enea.it (N. Cerone), jin.wang@hebut.edu.cn (J. Wang).

internal combustion engines. Gasification reactors can be categorized based on their design as fixed bed (updraft, downdraft), fluidized bed and entrained flow gasifiers. Specifically, updraft gasifiers classification is related to the opposite inlet directions of the gas (from bottom) and feedstock (from top) flows. These are known to have high residence time and a low gas flow velocity that result in a very high carbon conversion efficiency. Additionally, updraft reactors have the capability of using biomass with a high moisture content to produce syngas with higher hydrogen yield compared to other gasifier designs. Updraft gasifiers can be further divided into the bottom-lit design, and top-lit design. The bottom-lit represents the conventional design where the char reacts at the grate, while at the top-lit gasifier the reaction zone is transferred to the top of the reactor which ensures the tar burning (Saravanakumar et al., 2007). The main flaw of the bottom-lit updraft gasifier is the high yield of tar (up to 20%), which indicates the necessity for a subsequent syngas cleaning procedure (Sikarwar et al., 2016). Operating parameters, such as biomass flow, gasifying agent, temperature and pressure of the reactor have a strong influence on the quality of the produced syngas and gasification performance. Further investigations on the influence of each operating parameter during biomass gasification process are always needed for the continuous development and optimization of gasifiers. Gasification modelling is of extreme importance since it can significantly reduce expensive and time-consuming experimental surveys. Generally, biomass gasification modelling can follow mainly three different routes: thermodynamic equilibrium model (TEM), chemical kinetics and artificial neural network (ANN) models (Patra and Sheth, 2015). The simplest approach is the TEM which considers that species can react with one another for an infinite amount of time when the equilibrium is reached. TEM approach describes the behaviour of gasification and oxidation processes through the minimization of Gibbs free energy, which calculates the chemical equilibrium of prescribed chemical species at a specific pressure and temperature (Ramos et al., 2019).

The development of biomass gasification models is connected to the one of coal gasification, since similar chemical processes occur. For this reason, it is worth mentioning the work of Cau et al. (2015) that modelled an updraft coal gasifier using a TEM model. The authors modelled the pyrolysis process using correlations obtained from the experimental final products for a specific coal. Their results indicated a high influence of air to coal and steam to coal mass ratios on the gasification process. They remarked a decrease in the heating value while increasing air to coal ratio due to the promotion of combustion reactions and consequently releasing more CO_2 instead of CO. Also, the increase of steam to coal ratio enhances the water gas shift reaction which indicates higher yields of H_2 and CO_2 in the produced syngas. de Mena et al. (2017), continued the research of Cau et al. (2015) and developed a TEM model for updraft biomass gasifier which was a separate unit of the Combined Heat and Power — CHP plant. With the developed model they calculated the syngas production to be later burned in an external combustion chamber. They concluded that biomass with a maximum moisture content of 60%, and 20% of ash content can be used in an updraft gasification process. In the work of Dhanavath et al. (2018), the influence of pure oxygen and steam as gasifying agents on the syngas composition was analysed. The authors determined the optimal steam to biomass ratio in the range from 0.3 to 0.7, where the H_2/CO ratio was in the range between 0.83 and 1. Optimization of the gasification process with a TEM model was performed in research by Sreejith et al. (2013). Steam to biomass ratio was varied to increase process efficiency and H_2 yields, which consequently increases the lower heating value (LHV). They determined the optimal steam to biomass ratio to be 0.8 with a correspondent efficiency of 56.5%.

In their model, CH_4 predictions deviated from the experimental data and they prescribed this issue to the difficulty of reaching the equilibrium state for a steam methane reforming reaction. Conventional TEM models can be improved by implementing additional empirical correlations and separate models for tar formation. In that way, Ghassemi and Shahsavan-Markadeh (2014) implemented an empirical equation which takes into account the carbon conversion efficiency, and the experimental tar yield quantity. A modified model improved the agreement of syngas composition predictions with the experimental data, while it was limited regarding CH_4 predictions.

Including a chemical kinetics routine into a TEM, both flexibility and accuracy improve but at the expense of the increased complexity. Yu and Smith (2018) implemented a kinetic model only for gasification and oxidation zones in an updraft gasifier, while Smith et al. (2019) performed a similar procedure for the downdraft gasifier. In both works, the TEM model was used for the pyrolysis zone. Modelling predictions were compared to the results obtained with the TEM models, and it was achieved a better agreement with the experiment by including the chemical kinetics routine, especially considering the amount of tar content detected in the produced syngas. The same combination of modelling approaches was used in the work of Cao et al. (2019). The authors numerically investigated the influence of air enrichment with O_2 to reduce the tar content in the produced syngas. The results indicated the limited capability of reducing the tar with air enrichment, and authors suggested the usage of a catalyst to improve the conversion of tar species. When modelling the updraft fixed bed gasification process, special focus needs to be given to the pyrolysis zone, since the light gaseous products outflow from the reactor, without reacting in the gasification zone. In the above mentioned studies, the pyrolysis modelling approach is based on correlations obtained from the experimental final products yields, which indicates a model dependence on the specific biomass composition and/or working conditions (de Mena et al., 2017). The inclusion of a pyrolysis kinetic model can overcome this issue. A biochemical analysis of biomass (cellulose, hemicellulose, lignin and extractives) is usually used as an input to the kinetic modelling approach. Gonzalez-Quiroga et al. (2017) reviewed several kinetic models giving emphasis to the secondary gas-phase reaction mechanisms. The authors concluded that detailed mechanisms for cellulose and lignin reactions are developed, but recommend further improvements of the hemicellulose reactions. Researchers from Politecnico di Milano have developed a multi-step kinetic model for complete coal (Corbetta et al., 2015) and biomass (Ranzi et al., 2014) gasification process and applied it to various types of gasifier designs. When modelling updraft gasifiers the authors achieved accurate temperature profiles and concluded that the model could predict the temperature in places where installing a thermocouple could be difficult. The same principle was used in the work of Corbetta et al. (2014), where a kinetic pyrolysis model of centimetre-scale biomass was developed and validated over various operating conditions. The comparison between predictions and experimental results indicated a good ability of the model in predicting pyrolysis products of thermally thick particles. Further model development and modifications are possible through the optimization of the chemical kinetic parameters.

Considering findings from the literature, the objective of this work is to propose a new model approach for the bottom-lit updraft gasification process that benefits from the combination of a kinetic model for the pyrolysis zone and a TEM model for the gasification and oxidation zones. The proposed approach will be more flexible regarding the operating conditions and types of biomass when compared to the available models that use TEM for the pyrolysis zone, while it will be less complex when

Fig. 1. Biomass feedstock — almond shells.

Table 1
Almond shells properties.

	Almond shells	Source
Bulk density, kg/m^3	417	
Moisture, wt.%	11.8	
Carbon, wt.%	47.9	
Hydrogen, wt.%	6.3	
Nitrogen, wt.%	0.4	Cerone and Zimbardi (2018)
Oxygen, wt.%	45.4	
Cellulose, wt.%	31.2	
Hemicellulose, wt.%	28	
Lignin, wt.%	32.18	
Ash, wt.%	1.2	
Lig-C, wt.%	4.18	
Lig-H, wt.%	21.67	Corbetta et al. (2014)
Lig-O, wt.%	6.33	
Hydrophobic extractives, wt.%	7.42	–

compared to the fully kinetic models. In the proposed model, the pyrolysis zone was modelled using the CRECK-S-BIO kinetic mechanism (Debiagi et al., 2015), and two different secondary gas-phase reaction mechanisms with distinct levels of complexity (Debiagi et al., 2016; Goyal and Pepiot, 2017), to evaluate the necessity of using a more detailed and complex kinetic mechanism. Char gasification and oxidation processes were modelled through the minimization of Gibbs free energy approach. The model was implemented in MATLAB using the Cantera reaction kinetics library (Goodwin, 2001).

2. Materials and methods

In this section biomass characteristics and experimental power plant with the considered operating conditions are firstly described. Afterwards, the used models are presented and a method to determine the prediction error is shown.

2.1. Biomass feedstock

In this research, almond shells (agricultural residue) were used as feedstock (see Fig. 1). The composition of biomass in terms of cellulose, hemicellulose, total lignin and ash (in dry basis) was taken from the literature (Cerone and Zimbardi, 2018). For modelling purposes, the composition of three structural lignins: lig-C, lig-H and lig-O, rich in carbon, hydrogen and oxygen, respectively, were also taken from the literature (Corbetta et al., 2014). The remaining share of the biomass composition was assumed to be hydrophobic extractives, due to the known high content of oils present in this specific type of feedstock. The summary of almond shells properties is listed in Table 1.

2.2. Experimental

The pilot-scale uPdRAft GAsifier (PRAGA plant) is an experimental rig placed at ENEA Trisaia Research Centre in southern Italy. Fig. 2 shows the PRAGA facility and a scheme of the gasifier. The main element of the plant is a 2.4 m high cylindrically shaped autothermic reactor with a diameter of 50 cm. The reactor walls are covered with a 10 cm thick insulation layer, which results in an effective reactor diameter of 30 cm. The bottom of the reactor is shaped like a cone, where the ash is collected and discharged at the end of experiments. Biomass is filled up to 1.3 m from the grate in a semi-continuous mode. The feeding

system transfers biomass with augers into the collecting chamber which opens every 12 min and biomass drops in the reactor under a nitrogen atmosphere to avoid gas leakage. This procedure introduced the variation of around 5% of the biomass bed height over time. The plant is capable of gasifying up to 20–30 kg/h of various types of feedstock, which are introduced at the upper part of the reactor. The facility is equipped with a compressor and a separate external boiler used to produce superheated steam. Various gasifying agents can be used in the process, such as air, enriched air, pure oxygen, steam, or a combination of each. Gasifying agents are introduced at the lower part of the reactor and flow in the counter-current direction of the biomass, which gives rise to the classification of updraft gasification. The gasification process occurs slightly above the atmospheric pressure. The temperature profile along the reactor is measured with a steel probe that contains 11 thermocouples placed at different heights. At the reactor's exit, the produced syngas can be directed through the scrubber for cleaning, cooling procedure and two coalescing filters for the drying process. The temperature measurement error is 1–2 degree in a range between 300 °C and 600 °C, while at temperatures above 600 °C the error is 2 degrees. The feeding system was calibrated to determine the feeding rate with a measurement error of 1%. Air, steam and synthesis gas flows were measured with an error of 1%. The composition of the produced syngas was analysed using a gas chromatograph (GC), HP 6890, which is equipped with thermal conductivity detector (TCD), where the standard deviation of measurement was 2% (Cerone et al., 2020). The liquid content was analysed by means of a filtered solution through gravimetric method. Aldehydes and short-chain acids were analysed using a high-performance liquid chromatography (HPLC) with standard deviations of 3% and 1%, respectively. Other organic molecules were analysed using a GC–mass spectrometry (MS), agilent model 5975 and agilent column DB5MS, with a standard deviation error between 1 and 5% (Cerone et al., 2016). A more detailed description of the PRAGA experimental facility and the used techniques can be found in Cerone and Zimbardi (2018).

2.3. Test conditions

With the emphasis of applying the model to various operating conditions, 11 different experimental cases were evaluated. The experimental data were taken from previous experimental campaigns (Cerone and Zimbardi, 2018; Cerone et al., 2020). The first three cases were carried out with air as gasifying agent, while in the remaining cases air and steam were used.

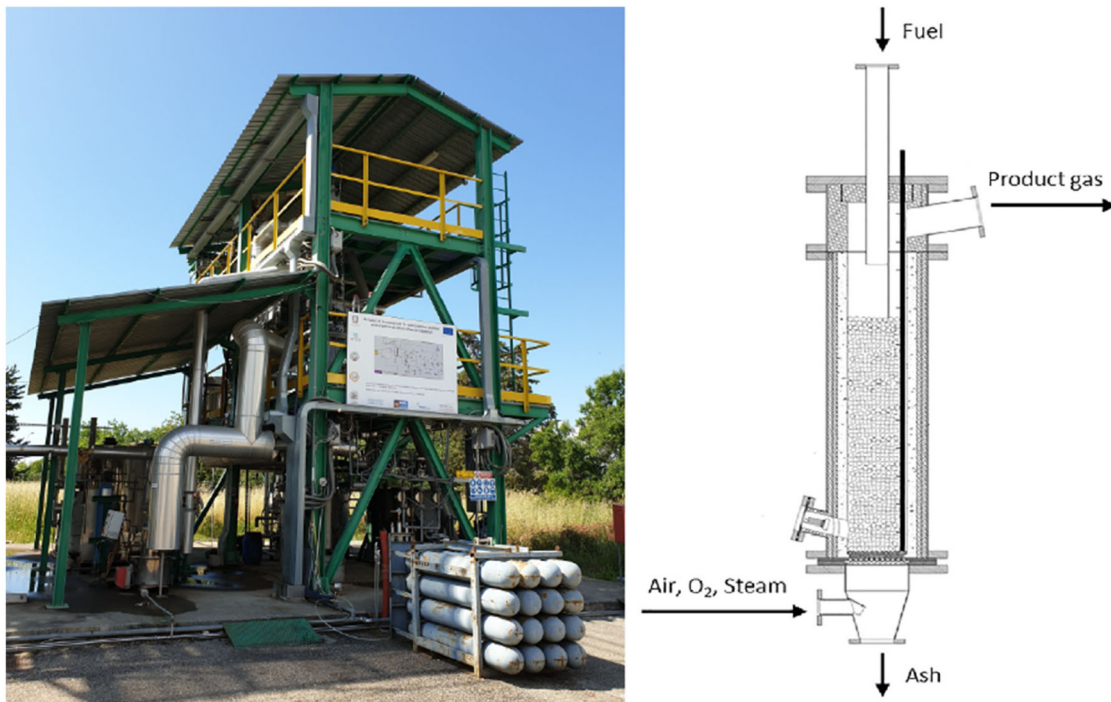Table 2 lists the operating conditions considered in each experiment.

Fig. 2. PRAGA plant (left) and the scheme of gasifier (Liakakou et al., 2019) (right).

Table 2
Operating conditions.

Experiment Code	Biomass, kg/h	Air, kg/h	Steam, kg/h	ER (O_2), -	ER (H_2O), -
A21	24.3	30.6	0	0.21	0
A24_1	12.4	16.7	0	0.24	0
A24_2	21.2	28.8	0	0.24	0
AS20/08	24.7	29.5	2	0.20	0.08
AS19/11	26.0	30.4	2.8	0.19	0.11
AS21/16	24.3	30.6	4	0.21	0.16
AS22/19	22.4	29.0	4	0.22	0.19
AS22/24	22.4	28.9	5	0.22	0.24
AS24/25	22.1	31.0	5.2	0.24	0.25
AS24/28	21.2	29.8	5.5	0.24	0.28
AS25/30	21.6	31.5	6	0.25	0.30

Equivalence ratios (ER) of oxidation (O_2) and change in water reaction (H_2O) were determined as follows:

$$ER(O_2) = \frac{feed\ O_2}{O_2\ needed\ for\ complete\ combustion} \quad (1)$$

$$ER(H_2O) = \frac{feed\ H_2O}{H_2O\ needed\ for\ complete\ reaction} \quad (2)$$

The temperature profiles are shown in Fig. 3. The dots in graphs denote positions of the temperature probes from the grate up to 1.3 m of the reactor. The shadowed area shown in Fig. 3, represents the pyrolysis zone. It is important to underline that its representation is merely qualitative since there can occur slight shifts depending on the case.

2.4. Pyrolysis modelling

A kinetic modelling tool, developed in the previous work (Ferreiro et al., 2017), was implemented in MATLAB using the CRECK-S-BIO mechanism (Debiagi et al., 2015), two different secondary gas-phase mechanisms (Debiagi et al., 2016; Goyal and Pepiot, 2017) and the Cantera reaction kinetics library (Goodwin, 2001). The species conservation and reaction rates were solved through a stiff ordinary differential equation (ODE) solver included in MATLAB (2019), where ultimately the final yields of the pyrolysis

products were determined. The conservation of each species was calculated as following (Wang et al.):

$$m\frac{dY_k}{dt} = \sum_k \dot{m}_{k,gen} \quad (3)$$

In Eq. (3), the term m stands for the total mass, Y_k is a mass fraction of kth specie and the $\dot{m}_{k,gen}$ represents the rate of generated mass of kth species, determined as follows:

$$\dot{m}_{k,gen} = \dot{\omega} \cdot M_{w,k}/\rho_{gas}, \quad (4)$$

where $M_{w,k}$ is the molecular weight of the kth specie and ρ_{gas} the gas density. The net production rates, $\dot{\omega}$ were calculated using the Arrhenius law:

$$k(T) = AT^\beta exp\left(-\frac{E}{RT}\right) \quad (5)$$

In the Arrhenius equation, A, β and E represent pre-exponential factor, temperature exponent and activation energy, respectively.

The experimental temperature profiles and the biochemical composition of biomass were used as model inputs. The CRECK-S-BIO kinetic mechanism (Debiagi et al., 2015) was used to describe the pyrolysis of almond shells. This mechanism considers that biomass is mainly composed of four organic components (cellulose, hemicellulose, lignin and extractives) that in a general
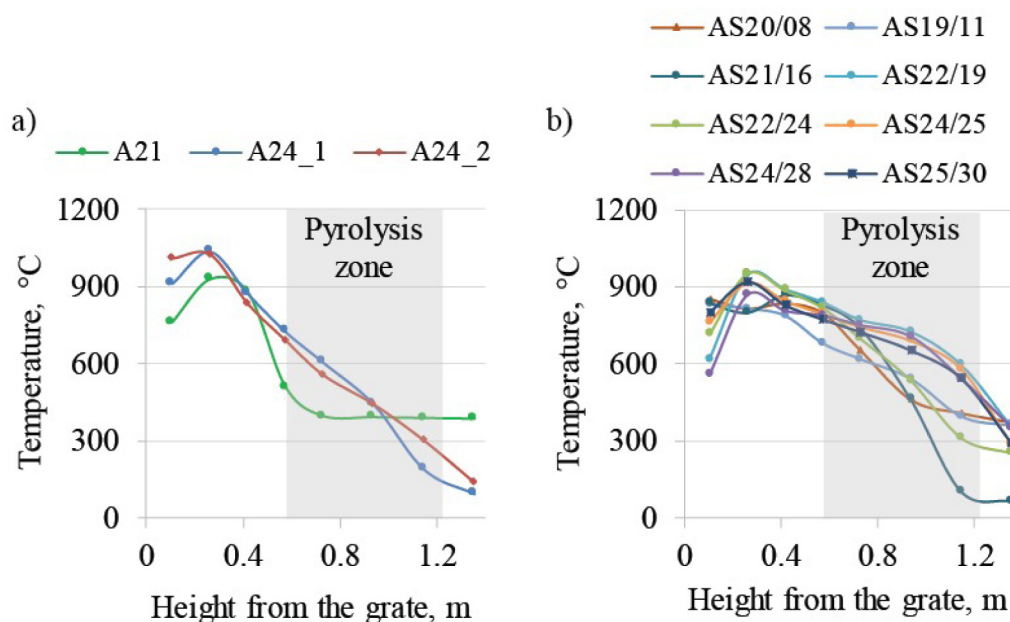
Fig. 3. Experimental temperature profiles for (a) air gasification, (b) air+steam gasification (Cerone and Zimbardi, 2018; Cerone et al., 2020).

way decompose into a solid phase (char), liquid species and non-condensable gases. The decomposition of the referred components is described through 27 chemical reactions that occur in parallel, considering 51 chemical species: 23 solid species, 22 condensable gases (tars, other liquids and H_2O) and 6 non-condensable gases. In this present work, the liquid species that resulted from biomass pyrolysis were divided into two groups: lighter and heavier species. The lighter species represent carbonyls and alcohols, while the heavier species are furans, sugars and phenolics as described in the work of Anca-Couce and Obernberger (2016). The secondary gas-phase reactions of the lighter species occurred during a shorter period, which is directly connected to the experimental gas residence time (Cerone and Zimbardi, 2018; Cerone et al., 2020), while the reactions of the heavier species occurred within a much longer period, which is related to the particle residence time (Cerone and Zimbardi, 2018; Cerone et al., 2020) due to the assumption that heavier tars were sticked to the solid particle. Two secondary gas-phase mechanisms with distinct levels of complexity were implemented to describe the secondary gas-phase reactions. First one is the detailed kinetic mechanism used in the work of Debiagi et al. (2016) that contains 137 chemical species and 4533 chemical reactions. The second one is a reduced kinetic mechanism proposed by Goyal and Pepiot (2017), which considers 44 chemical species and 118 chemical reactions. This latter mechanism was initially developed to be used under pyrolysis conditions, however, the authors concluded that it could provide good results when applied under gasification conditions. The updraft gasification process has higher content of liquid species in the producer gas. One of the reasons is the outflow of the liquids created in the pyrolysis zone of the reactor with the syngas flow. This event prevents liquid species to reach the gasification zone and, consequently, cracking at higher temperatures (Cerone et al., 2020). Hence, it is considered that only char enters the gasification and oxidation zones to react with the gasifying agents (Gordillo et al., 2009). A schematic representation of the proposed model is shown in Fig. 4.

To validate the biochemical composition of almond shells, thermogravimetric analysis (TGA7, Perkin Elmer, Waltham, MA, USA) was performed at a heating rate of 10 °C/min from 60 °C up to 800 °C, under an inert atmosphere of nitrogen.

Table 3
Main biomass gasification reactions (Dhanavath et al., 2018; Gordillo et al., 2009).

Reaction no.	Reaction name	Reaction
Heterogeneous reactions		
R1	Carbon combustion	$C + O_2 \rightarrow CO_2$
R2	Carbon partial combustion	$C + 0.5O_2 \rightarrow CO$
R3	Boudouard reaction	$C + CO_2 \rightarrow 2CO$
R4	Water-gas reaction	$C + H_2O \leftrightarrow CO + H_2$
R5	Methanation	$C + 2H_2 \rightarrow CH_4$
Homogeneous reactions		
R6	CO combustion	$CO + 0.5O_2 \leftrightarrow CO_2$
R7	Water-gas shift reaction	$CO + H_2O \leftrightarrow CO_2 + H_2$
R8	Steam methane reforming	$CH_4 + H_2O \leftrightarrow CO + 3H_2$

2.5. Char gasification and oxidation model

To ensure the simplicity of the model, char gasification and oxidation were modelled using a TEM that calculates the thermochemical equilibrium through the minimization of Gibbs free energy. Within this purpose, the Cantera chemical equilibrium Gibbs solver (equilibrate method) was included in the kinetic tool referred to in the previous section. This subroutine can determine the chemical equilibrium concentration of a mixture of species, holding two thermodynamic properties fixed at their initial values. The main assumption of this approach is the long residence time of the biomass particles inside of these types of reactors that can almost ensure chemical equilibrium. Therefore, this approach is suitable for modelling the gasification process in a fixed bed reactor (Chen et al., 2013).

The model inputs are experimental pressure and temperature of the gasification process, mass fractions of the gasifying agents and chemical species obtained from the pyrolysis zone output as shown in Fig. 4. To ease the discussion of the results, the main biomass gasification reactions are listed in Table 3. In the TEM model, 100% carbon conversion efficiency was assumed due to the long residence time of solid particles in the reactor, as was observed in the experimental results (Cerone and Zimbardi, 2018).
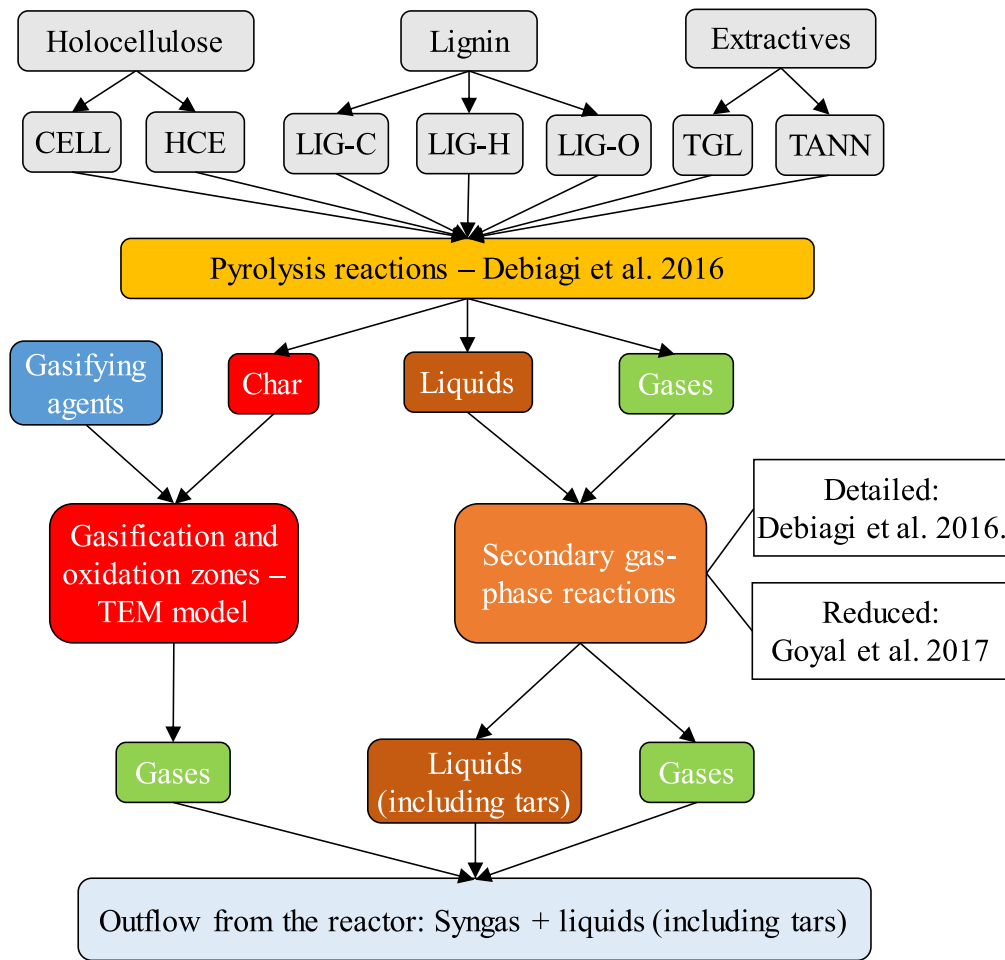
Fig. 4. Schematic representation of the proposed model.

2.6. Error function

To evaluate the prediction accuracy, average prediction errors (APE) of the major gas species from air and air + steam gasification process in relation to the experimental data were calculated using the following equation:

$$APE = \frac{\sum_i^N \left| \frac{\varphi_{p,i} - \varphi_{e,i}}{\varphi_{e,i}} \right|}{N} \cdot 100 \tag{6}$$

where $\varphi_{p,i}$ and $\varphi_{e,i}$ represent the predicted and experimental volume fraction of a specific gaseous species (H_2, CO, CO_2 and C_nH_m) for ith experimental case, while N is the total number of cases.

3. Results and discussion

The results and discussion section is divided into five subsections. Firstly, the predicted mass loss profile is compared to the experimental data. Later, pyrolysis model results are presented to determine the inputs for the TEM model. Afterwards, the final syngas compositions are analysed for air and air+steam gasification, while at the end the average prediction errors are shown.

3.1. Mass loss profiles

Fig. 5 shows the comparison between the experimental and predicted weight loss profiles for almond shells pyrolysis, using a
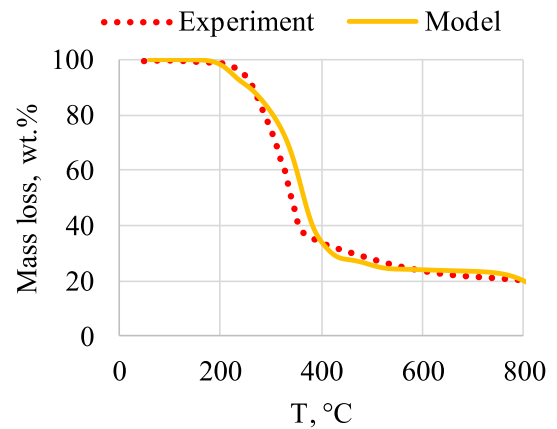

Fig. 5. Experimental and predicted mass loss profiles of almond shells.

heating rate of 10 °C/min. It is visible that the predicted weight loss curve follows the measurements data, achieving satisfying accuracy, hence, it can be concluded that the biochemical composition of almond shells retrieved from literature can be used as the model input.

3.2. Pyrolysis zone

Pyrolysis products for the observed cases are shown in Fig. 6. Since the temperature profiles are quite similar in all cases (c.f.
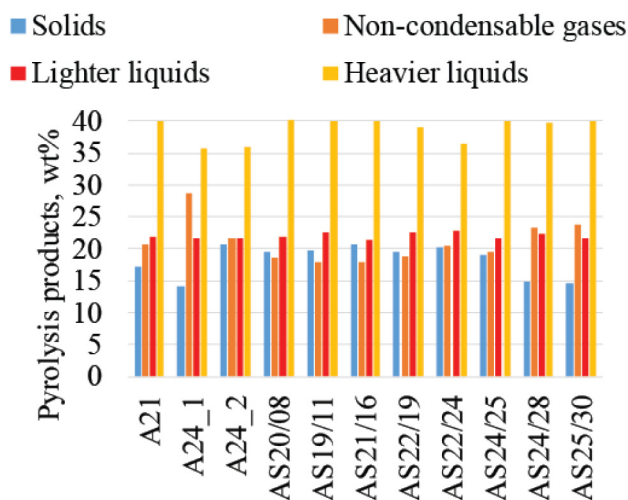
Fig. 6. Biomass pyrolysis products.

Fig. 7. Predicted and experimental liquid content.

Fig. 3), it is expected to also obtain similar results. The exception is the case A24_1 due to the much lower biomass flow compared to other cases (see Table 2), which results in a much higher particle residence time. For instance, the residence time of the case A24_2 is 1.64 h while for the case A24_1 is 2.81 h. This explains the fact that in the case A24_1 the final char yield is 14%, while in the remaining cases the share of char is higher. Fig. 5 also shows that the increase in the residence time also led to the formation of a higher amount of non-condensable gases in the case A24_1 when compared to other cases.

Due to the reactor configuration (updraft gasifier), as was already mentioned, the lighter liquid species reacted at the gas residence time within the secondary gas-phase reactions, while the heavier species, being sticked with the solid particles, were subject to a longer pyrolysis residence time. After the completion of this stage, all the remaining condensable gases (liquids) out-flow from the reactor. To determine the boundary between the pyrolysis and gasification zones, the maximum pyrolysis temperature was determined by matching the predicted liquids content at a given temperature to obtained correspondent experimental values (Cerone and Zimbardi, 2018; Cerone et al., 2020). When the prediction error of liquid content was below 10%, the current temperature was chosen as a boundary between the two zones. Fig. 7 shows the comparison between predicted and experimental liquid contents.

The predicted char resultant from the pyrolysis zone and mass fractions of the gasifying agents were used as inputs to the TEM model to predict the formation of syngas in the gasification and oxidation zones.

3.3. Air gasification

The analysis of the gasification process with air as gasifying agent is performed on three experimental cases. Fig. 8 shows the comparison between the measurements and predictions of the main gas species volume fractions.

Focusing first on the A21 and A24_2 cases, it is observed that increasing the $ER(O_2)$ from 0.21 to 0.24 results in the increase of the CO_2 yield at the expense of CO. Increasing the $ER(O_2)$ indicates that more oxygen is present in the system, which shifts the reaction R1 to the right. It is important to notice that the CO_2 gradient is higher than the CO gradient, which leads to a further increase of CO_2 yields. This behaviour was already observed for updraft gasification in the work of Chen et al. (2013). In the
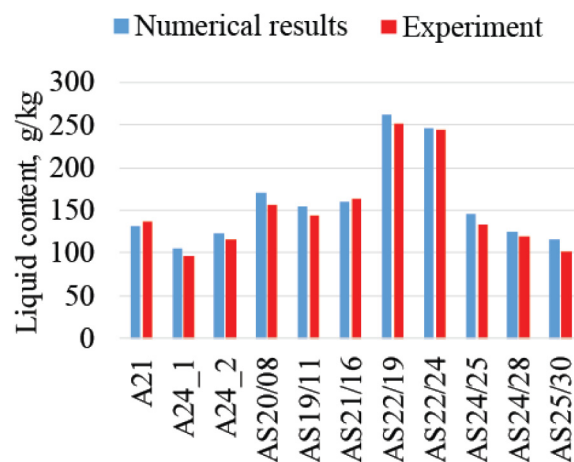
present work, as observed in Fig. 6, both models can predict this trend. Additionally, higher $ER(O_2)$ results in lower C_nH_m yields, feature that is captured by both mechanisms. Changing the $ER(O_2)$ has a minor effect on the H_2 yields, which can be also noticed in the predictions obtained with the detailed mechanism. This behaviour was observed in the experimental measurements and also in previous work (de Mena et al., 2017).

To analyse the influence of the biomass flow on the syngas composition, cases A24_1 and A24_2 were conducted maintaining the same $ER(O_2)$. According to the experimental data, higher biomass flow (lower residence times) should decrease the CO and increase the CO_2, but predictions indicate the opposite trend. This issue can be prescribed to the assumption of thermo-chemical equilibrium in gasification and oxidation zones. Due to the lower amount of char in case A24_1 (see Fig. 6) and the same amount of oxygen from air input (as in case A24_2), much more CO_2 is predicted in A24_1 case, as shown in Fig. 8. On the other hand, measurements show that increasing the biomass flow slightly increases the H_2 yield, a feature that is captured by predictions using both mechanisms. This can be again addressed to the higher amount of char in the case A24_2, which indicates a higher H_2 content captured in solid char that enters the gasification and oxidation zones. Afterwards, the H_2 is released from solid char at higher temperature due to the assumption of thermo-chemical equilibrium.

H_2/CO volume fraction ratio is shown in Fig. 9(a). Generally, the predictions obtained with both secondary gas-phase mechanisms achieved a similar trend as experimental data for all cases. Although, the detailed chemical mechanism achieved a better agreement with the experimental data. The change of $ER(O_2)$ does not have a strong influence on the H_2/CO ratio, which is visible by comparing the A21 and A24_2 cases. This is mainly because higher $ER(O_2)$ results in decreasing both H_2 and CO yield, which will maintain the similar value of the ratio. A comparable behaviour was also noticed in the work of Saha et al. (2019). Observing the two cases with $ER(O_2) = 0.24$, it can be noticed that higher residence times (A24_1) decrease the H_2/CO ratio, which is captured by the predictions with both secondary gas-phase mechanisms.

Fig. 9(b) shows the variation of the CO/CO_2 ratio with $ER(O_2)$. It is observed a slight decrease in the results due to mainly the occurrence of reaction R1. Also, due to the before mentioned under predicted CO_2 yields in the case A24_2, the opposite behaviour of the CO/CO_2 ratio is observed in the predicted results when compared to the measurements.
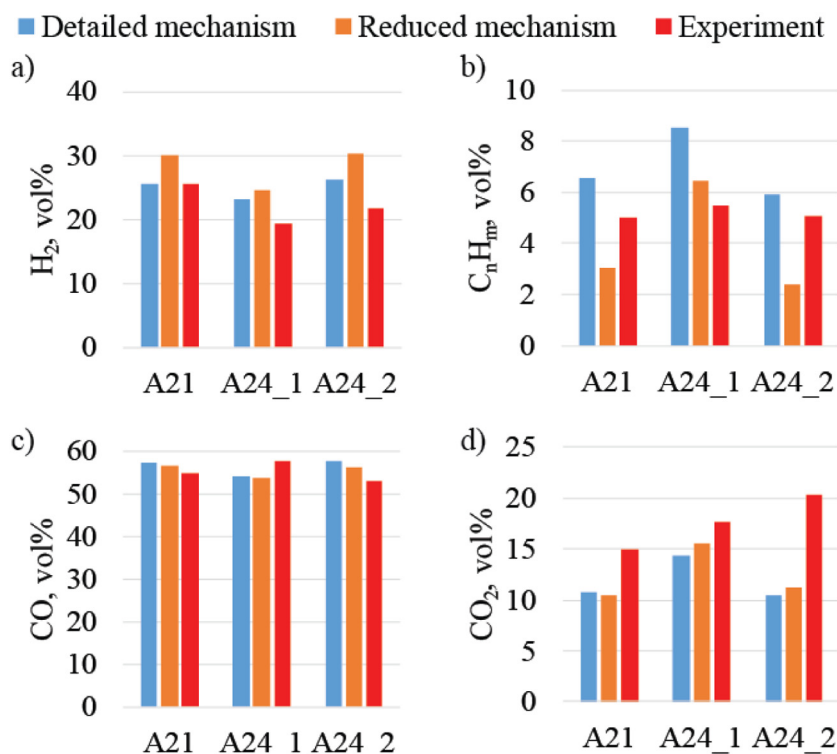
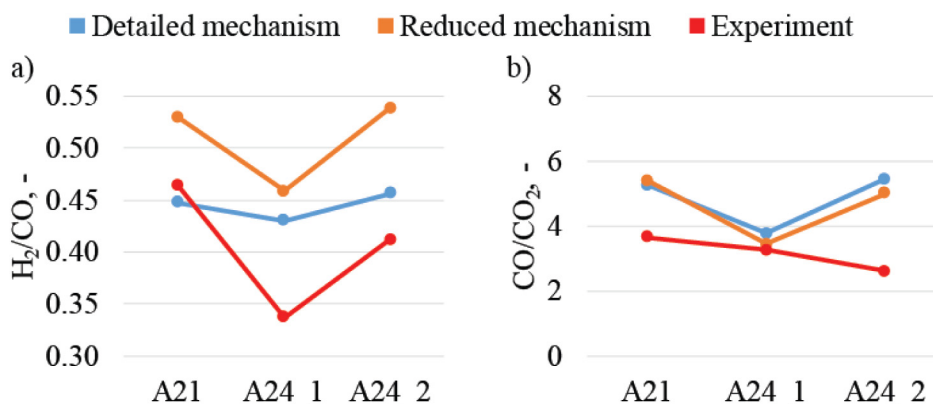**Fig. 8.** Syngas composition comparison for air gasification.

Fig. 9. Syngas compositional parameters for air gasification.

3.4. Air and steam gasification

ER(H_2O) has a strong influence on the water-gas reaction (R4) and water-gas shift reaction (R7) which represent the most important reactions in gasification with steam (Cao et al., 2021). In Fig. 10 volume fractions for 8 experimental cases are shown, lined up from the lowest ER(H_2O) to the highest. Since the ER(O_2) is not constant in all cases, reactions R1, R2 and R6 also play important roles in the results discussion.

By increasing the ER(H_2O), reactions R4 and R7 enhance the H_2 yield by adding more steam into the system, which is consistent with previous findings (Ferreiro et al., 2020). Although, at some point H_2 reaches its maximum and remains at similar values by further increasing ER(H_2O). This can be addressed to the parallel increasing of ER(O_2) that slightly decreases the H_2 yield. This behaviour can be noticed in the presented results where both secondary gas-phase mechanisms follow the experimental data. A similar change of H_2 yield by varying the ER(H_2O) was recorded in a work by Dhanavath et al. (2018).

While observing CO and CO_2 volume fractions, it is important to analyse cases AS19/11, AS21/16 and AS22/19. In these cases, ER(O_2) and ER(H_2O) increase from 0.19 and 0.11 to 0.22 and 0.19, respectively. Usually, higher ER(O_2) indicates the increase of CO_2 at the expense of decreasing the CO, because more oxygen in the system shifts the reaction R1 to the right. Although in the observed cases, the situation is quite opposite. The experimental case with the highest ER(O_2) indicates the highest CO yield. This can be addressed to the strong influence of Boudouard reaction (R3) and water-gas reaction (R4) at lower values of ER(O_2) and ER(H_2O). Predictions are not following this behaviour due to the assumption of thermodynamic equilibrium in the gasification and oxidation zones, which underpredict the influence of R3 and R4 reactions. At higher values of ER(O_2) and ER(H_2O), CO_2 starts to increase at the expense of CO and the predicted results were able to capture this trend accurately. Increasing the ER(O_2) and ER(H_2O) slightly affects the C_nH_m yields, and the predictions can capture the tendencies of the measurements. Similar results were
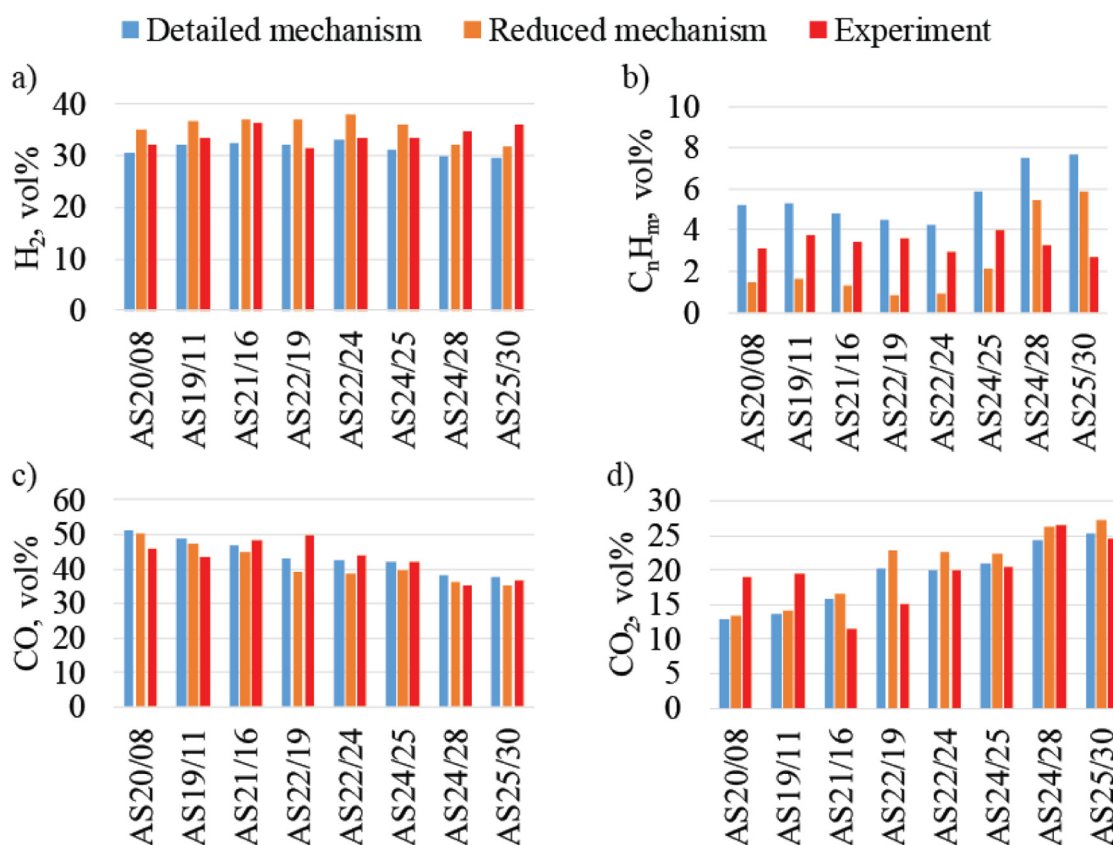
Fig. 10. Syngas composition comparison for air and steam gasification.

obtained in previous works when using the kinetic model by Cao et al. (2021) and the TEM model by Dhanavath et al. (2018).

H_2/CO and CO/CO_2 ratios for different $ER(O_2)$ and $ER(H_2O)$ are shown in Fig. 11. As it can be seen, increasing the equivalence ratios has a generally positive effect on the H_2/CO ratio. Although, the lowest H_2/CO ratio is observed for the case AS22/19, which can be prescribed to the high amount of CO in this case, as already mentioned. A positive effect of $ER(H_2O)$ on the H_2/CO ratio was already observed in a work by Dhanavath et al. (2018).

Observing the CO/CO_2 ratio, it can be noticed that by increasing the equivalence ratios, a decrease of CO/CO_2 is noted, which is due to the increasing of the CO_2 yields. Also, experimental data indicated a significant rise of CO/CO_2 ratio in cases AS21/16 and AS22/19, which is related to the higher CO and much lower CO_2 yields than what would be expected when increasing the $ER(O_2)$. The predicted results were not able to capture this behaviour.

3.5. Prediction error

In this section, the model validation concerning the major gas species will be presented and discussed through the APE values.

Table 4 shows the APE of major gas species from the air and air + steam gasification process in relation to the experimental data, for both secondary gas-phase mechanisms.

Generally, results obtained using the more detailed secondary gas-phase mechanism showed a much better agreement with the experimental data for air gasification, which shows the necessity of using detailed mechanisms to improve predictions accuracy. However, CO seems to be an exception, which is predicted with an APE below 10% for both mechanisms. On the other hand, both mechanisms can predict the yields of H_2, CO and CO_2 with good accuracy for gasification with air and steam.

When observing C_nH_m prediction errors, much higher deviations can be noticed for both secondary gas-phase mechanisms. This is because, in the presented model, the C_nH_m yields are from the pyrolysis zone due to the limitation of the TEM model in predicting C_nH_m in the gasification zone (Ghassemi and Shahsavan-Markadeh, 2014). Since the liquids mostly crack at higher temperatures (above 1000 K) (Gordillo et al., 2009), the maximum temperature in the pyrolysis zone highly influences the amount of the produced C_nH_m. For that reason, choosing the boundary between the pyrolysis and gasification zones is one of the main factors for accurate C_nH_m predictions. It can be observed that the detailed mechanism over predicts the C_nH_m yields, and this phenomena was already noticed by other authors, when using the kinetic model for solving gas-phase reactions (Umeki et al., 2010). Hence, higher errors of C_nH_m are considered acceptable due to the much lower C_nH_m volume fraction when compared to other gases (CO, CO_2 and H_2) (Smith et al., 2019). On the other hand, the reduced mechanism highly under predicts the C_nH_m, mostly due to the lack of chemical reactions that can consider the thermal-cracking of liquids with oxygen and steam.

4. Conclusion

In this study, the gasification process of almond shells carried out in a pilot-scale updraft gasifier was modelled using a combination of a kinetic mechanism with a TEM model. Model predictions were compared to the experimental data for 3 cases of air gasification and 8 cases for air and steam gasification. The experimental data were retrieved from previous experimental campaigns. Also, the mass loss profile, using the same experimental TGA operating conditions, was predicted to validate the reliability of the biomass biochemical composition. Firstly, biomass decomposition, as a first stage of the pyrolysis kinetic model,
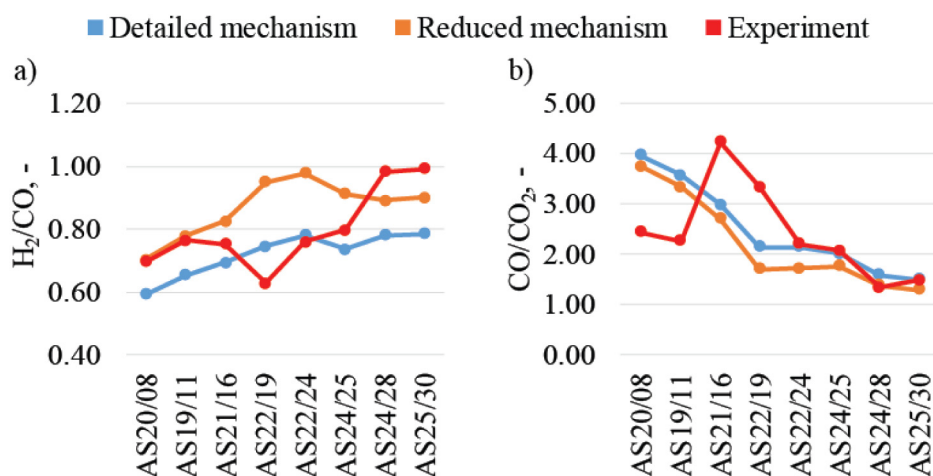
Fig. 11. Syngas H_2/CO and CO/CO_2 ratios for air and steam gasification.

Table 4
Average prediction errors of syngas composition and tar content.

Gas	Secondary gas-phase reaction mechanism	Air gasification	Air+steam gasification
H_2, %	Detailed	13.58	7.81
	Reduced	27.85	10.14
CO, %	Detailed	6.37	6.90
	Reduced	5.55	8.83
CO_2, %	Detailed	31.47	18.10
	Reduced	28.86	23.51
C_nH_m, %	Detailed	33.97	72.62
	Reduced	36.29	68.85

was described using the CRECK-S-BIO kinetic mechanism to determine the inputs that were used in the secondary gas-phase reactions mechanisms and in the TEM model. Secondary gas-phase reactions were modelled using the two mechanisms with distinct levels of complexity. Gasification and oxidation processes were modelled applying a thermodynamic equilibrium model based on the minimization of Gibbs free energy.

The predictions obtained with the detailed secondary gas-phase mechanism generally showed a better agreement with measurements. Nevertheless, predictions obtained using both mechanisms achieved good accuracy for H_2 and CO predictions for air and steam gasification, mostly with an average prediction error below 10%. However, for the CO_2 predictions higher deviations were observed (around 20%), mainly due to the assumption of thermodynamic equilibrium in the gasification and oxidation zones. The reduced mechanism showed generally higher deviations for the predictions of H_2, CO and CO_2 predictions, which is ascribed to the lack of chemical reactions that consider the thermal-cracking of liquids with oxygen and steam. Higher deviations were noticed for C_nH_m predictions regardless the mechanism. These preliminary results show that a detailed mechanism facilitates higher accuracy of the predicted results. Additionally, the modelling approach used in the present work is able to capture the gasification trends of the measurements obtained in an updraft gasifier and represents a good basis for further development.

CRediT authorship contribution statement

Damijan Cerinski: Writing - original draft, Methodology, Software, Writing - review & editing. **Ana Isabel Ferreiro:** Writing - original draft, Methodology, Reviewing and editing. **Jakov

Baleta: Supervision, Visualization, Investigation, Conceptualization. **Mário Costa:** Supervision. **Francesco Zimbardi:** Conceptualization, Writing - review & editing. **Nadia Cerone:** Conceptualization, Writing - review & editing. **Jin Wang:** Visualization, Writing - review & editing.

Declaration of competing interest

The authors declare that they have no known competing financial interests or personal relationships that could have appeared to influence the work reported in this paper.

References

Anca-Couce, A., Obernberger, I., 2016. Application of a detailed biomass pyrolysis kinetic scheme to hardwood and softwood torrefaction. Fuel 167, 158–167, https://doi.org/10.1016/j.fuel.2015.11.062.

Cao, Y., Bai, Y., Du, J., 2021. Air-steam gasification of biomass based on a multi-composition multi-step kinetic model: A clean strategy for hydrogen-enriched syngas production. Sci. Total Environ. 753, 141690, https://doi.org/10.1016/j.scitotenv.2020.141690.

Cao, Y., Wang, Q., Du, J., Chen, J., 2019. Oxygen-enriched air gasification of biomass materials for high-quality syngas production. Energy Convers. Manage. 199, https://doi.org/10.1016/j.enconman.2019.05.054.

Cau, G., Tola, V., Pettinau, A., 2015. A steady state model for predicting performance of small-scale up-draft coal gasifiers. Fuel 152, 3–12, https://doi.org/10.1016/j.fuel.2015.03.047.

Cerone, N., Zimbardi, F., 2018. Gasification of agroresidues for syngas production. Energies 11, 1280, https://doi.org/10.3390/en11051280.

Cerone, N., Zimbardi, F., Contuzzi, L., Baleta, J., Cerinski, D., Skvorčinskiene, R., 2020. Experimental investigation of syngas composition variation along updraft fixed bed gasifier. Energy Convers. Manage. 221, 113116, https://doi.org/10.1016/j.enconman.2020.113116.

Cerone, N., Zimbardi, F., Villone, A., Strjiugas, N., Kiyikci, E.G., 2016. Gasification of wood and torrefied wood with air, oxygen, and steam in a fixed-bed pilot plant. Energy Fuels 30, 4034–4043, https://doi.org/10.1021/acs.energyfuels.6b00126.

Chen, C., Jin, Y.Q., Yan, J.H., Chi, Y., 2013. Simulation of municipal solid waste gasification in two different types of fixed bed reactors. Fuel 103, 58–63, https://doi.org/10.1016/j.fuel.2011.06.075.

Corbetta, M., Bassani, A., Manenti, F., Pirola, C., Maggio, E., Pettinau, A., et al., 2015. Multi-scale kinetic modeling and experimental investigation of syngas production from coal gasification in updraft gasifiers. Energy Fuels 29, 3972–3984, https://doi.org/10.1021/acs.energyfuels.5b00648.

Corbetta, M., Frassoldati, A., Bennadji, H., Smith, K., Serapiglia, M.J., Gauthier, G., et al., 2014. Pyrolysis of centimeter-scale woody biomass particles: Kinetic modeling and experimental validation. Energy Fuels 28, 3884–3898, https://doi.org/10.1021/ef500525v.

de Mena, B., Vera, D., Jurado, F., Ortega, M., 2017. Updraft gasifier and ORC system for high ash content biomass: A modelling and simulation study. Fuel Process Technol. 156, 394–406, https://doi.org/10.1016/J.FUPROC.2016.09.031.

Debiagi, P.E.A., Gentile, G., Pelucchi, M., Frassoldati, A., Cuoci, A., Faravelli, T., et al., 2016. Detailed kinetic mechanism of gas-phase reactions of volatiles released from biomass pyrolysis. Biomass Bioenergy 93, 60–71, https://doi.org/10.1016/j.biombioe.2016.06.015.

Debiagi, P.E.A., Pecchi, C., Gentile, G., Frassoldati, A., Cuoci, A., Faravelli, T., et al., 2015. Extractives extend the applicability of multistep kinetic scheme of biomass pyrolysis. Energy Fuels 29, 6544–6555, https://doi.org/10.1021/acs.energyfuels.5b01753.

Dhanavath, K.N., Shah, K., Bhargava, S.K., Bankupalli, S., Parthasarathy, R., 2018. Oxygen–steam gasification of karanja press seed cake: Fixed bed experiments, ASPEN plus process model development and benchmarking with saw dust, rice husk and sunflower husk. J. Environ. Chem. Eng. 6, 3061–3069, https://doi.org/10.1016/J.JECE.2018.04.046.

Farzad, S., Mandegari, M.A., Görgens, J.F., 2016. A critical review on biomass gasification, co-gasification, and their environmental assessments. Biofuel Res. J. 3, 483–495, https://doi.org/10.18331/BRJ2016.3.4.3.

Ferreiro, A.I., Giudicianni, P., Grottola, C.M., Rabaçal, M., Costa, M., Ragucci, R., 2017. Unresolved issues on the kinetic modeling of pyrolysis of woody and nonwoody biomass fuels. Energy Fuels 31, 4035–4044, https://doi.org/10.1021/acs.energyfuels.6b03445.

Ferreiro, A.I., Segurado, R., Costa, M., 2020. Modelling soot formation during biomass gasification. Renew. Sustain. Energy Rev. 134, 110380, https://doi.org/10.1016/j.rser.2020.110380.

Ghassemi, H., Shahsavan-Markadeh, R., 2014. Effects of various operational parameters on biomass gasification process; a modified equilibrium model. Energy Convers. Manag. 79, 18–24, https://doi.org/10.1016/j.enconman.2013.12.007.

Gonzalez-Quiroga, A., Van Geem, K.M., Marin, G.B., 2017. Towards first-principles based kinetic modeling of biomass fast pyrolysis. Biomass Convers. Biorefinery 7, 305–317, https://doi.org/10.1007/s13399-017-0251-0.

Goodwin, D.G., 2001. Cantera User's Guide Fortran Version Release 1.2.

Gordillo, G., Annamalai, K., Carlin, N., 2009. Adiabatic fixed-bed gasification of coal, dairy biomass, and feedlot biomass using an air-steam mixture as an oxidizing agent. Renew. Energy 34, 2789–2797, https://doi.org/10.1016/j.renene.2009.06.004.

Goyal, H., Pepiot, P., 2017. A compact kinetic model for biomass pyrolysis at gasification conditions. Energy Fuels 31, 12120–12132, https://doi.org/10.1021/acs.energyfuels.7b01634.

Ishaq, H., Dincer, I., 2020. A new energy system based on biomass gasification for hydrogen and power production. Energy Rep. 6, 771–781, https://doi.org/10.1016/j.egyr.2020.02.019.

Liakakou, E.T., Vreugdenhil, B.J., Cerone, N., Zimbardi, F., Pinto, F., André, R., et al., 2019. Gasification of lignin-rich residues for the production of biofuels via syngas fermentation: Comparison of gasification technologies. Fuel 251, 580–592, https://doi.org/10.1016/j.fuel.2019.04.081.

2019. MATLAB and Optimization ToolboxTM Release R2019a.

Patra, T.K., Sheth, P.N., 2015. Biomass gasification models for downdraft gasifier: A state-of-the-art review. Renew. Sustain. Energy Rev. 50, 583–593, https://doi.org/10.1016/J.RSER.2015.05.012.

Ramos, A., Monteiro, E., Rouboa, A., 2019. Numerical approaches and comprehensive models for gasification process: A review. Renew. Sustain. Energy Rev. 110, 188–206, https://doi.org/10.1016/J.RSER.2019.04.048.

Ranzi, E., Corbetta, M., Manenti, F., Pierucci, S., 2014. Kinetic modeling of the thermal degradation and combustion of biomass. Chem. Eng. Sci. 110, 2–12, https://doi.org/10.1016/j.ces.2013.08.014.

Saha, P., Uddin, M.Helal., Toufiq Reza, M., 2019. Helal uddin m toufiq reza m a steady-state equilibrium-based carbon dioxide gasification simulation model for hydrothermally carbonized cow manure. Energy Convers. Manage. 191, 12–22, https://doi.org/10.1016/j.enconman.2019.04.012.

Saravanakumar, A., Haridasan, T.M., Reed, T.B., Bai, R.K., 2007. Experimental investigation and modelling study of long stick wood gasification in a top lit updraft fixed bed gasifier. Fuel 86, 2846–2856, https://doi.org/10.1016/j.fuel.2007.03.028.

Sikarwar, V.S., Zhao, M., Clough, P., Yao, J., Zhong, X., Memon, M.Z., et al., 2016. An overview of advances in biomass gasification. Energy Environ. Sci. 9, 2939–2977, https://doi.org/10.1039/C6EE00935B.

Smith, J.D., Alembath, A., Al-Rubaye, H., Yu, J., Gao, X., Golpour, H., 2019. Validation and application of a kinetic model for downdraft biomass gasification simulation. Chem. Eng. Technol. 42, 2505–2519, https://doi.org/10.1002/ceat.201900304.

Sreejith, C.C., Muraleedharan, C., Arun, P., 2013. Thermo-chemical analysis of biomass gasification by gibbs free energy minimization model-part: II (optimization of biomass feed and steam to biomass ratio). Int. J. Green Energy 10, 610–639, https://doi.org/10.1080/15435075.2012.709203.

Umeki, K., Yamamoto, K., Namioka, T., Yoshikawa, K., 2010. High temperature steam-only gasification of woody biomass. Appl. Energy 87, 791–798, https://doi.org/10.1016/j.apenergy.2009.09.035.

Wang, G., Silva, R., Azevedo, J., Martins-Dias, S., Costa, M., Cantera reactor class. (Accessed 22 December 2020).

Yu, J., Smith, J.D., 2018. Validation and application of a kinetic model for biomass gasification simulation and optimization in updraft gasifiers. Chem. Eng. Process - Process Intensif 125, 214–226, https://doi.org/10.1016/J.CEP.2018.02.003.

Zappa, W., Junginger, M., van den Broek, M., 2019. Is a 100% renewable European power system feasible by 2050? Appl. Energy 1027–1050, https://doi.org/10.1016/j.apenergy.2018.08.109.